Journal of Supramolecular Structure 2:558–581 (1974)

CALCIUM EFFLUX FROM INTERNALLY DIALYZED SQUID AXONS: THE INFLUENCE OF EXTERNAL AND INTERNAL CATIONS

M. P. Blaustein, J. M. Russell,* and P. De Weer

Department of Physiology and Biophysics, Washington University School of Medicine, St. Louis, Missouri 63110

Internal dialysis techniques have been used to examine the influence of external and internal cations on Ca efflux from ATP-depleted squid axons. The main observation is that Ca efflux is promoted by external Na and inhibited by internal Na. The Na_o-dependent Ca efflux appears to be a function of $[Na]_o^3$, and is also affected by the membrane potential; a 25 mV depolarization may cause as much as an e-fold decrease in Ca efflux. These data are consistent with a counter-transport exchange of $3Na^+$–for–$1Ca^{2+}$. A Ca_o-dependent Ca efflux has also been observed; it is prominent in Na sea water or Li sea water, and is markedly diminished in choline sea water. This flux is consistent with the idea of a Ca-Ca exchange diffusion process. Taken together, the Na_o- and the Ca_o-dependent Ca effluxes fit a two-site model for carrier-mediated Ca transport; one site binds two Na^+ or one Ca^{2+}, while the second site can bind either one Na^+ or one Li^+. The data reported here suggest that both sites must be filled on the inward journey, but that only the Ca-binding site need be occupied on the outward journey of the carrier. A mechanism of this type could derive sufficient energy from the Na and voltage gradients to maintain a $[Ca^{2+}]_o/[Ca^{2+}]_i$ concentration ratio of about 10^4 in the absence of ATP. The present experiments do not, however, rule out the possible participation of a metabolically driven Ca transport mechanism in vivo.

INTRODUCTION

It is now widely appreciated that calcium ions are not distributed at electrochemical equilibrium across the surface membranes of most (if not all) animal cells (cf 1). Furthermore, in cells where it has been measured, the concentration of free, ionized Ca ($[Ca^{2+}]_i$) is normally only a small fraction of the total intracellular Ca ($[Ca_T]_i$). This has been well

*Present address: Department of Physiology and Biophysics, University of Texas Medical Branch, Galveston, Texas 77550

documented in the squid giant axon where electrophoretic mobility (2) and diffusion coefficient measurements (2, 3) indicate that, of the 0.4 mM total Ca in squid axoplasm, less than 2% is free (i.e., $[Ca^{2+}]_i < 8 \times 10^{-6}$ M or pCa§ > 5.1). A more precise estimate of pCa was obtained by Katz and Miledi (4), who found that the suppression potential for transmitter release at the squid giant synapse is about +130mV; this potential is presumably a measure of the Ca equilibrium potential E_{Ca}, which is given by:

$$E_{Ca} = \frac{RT}{2F} \ln \frac{[Ca^{2+}]_o}{[Ca^{2+}]_i}$$

so that pCa is about 6.4 when the axon is bathed in sea water containing 11 mM Ca. Another measure of $[Ca^{2+}]_i$ was obtained by Baker et al. (5), using the photoprotein aequorin, which emits light in the presence of ionized Ca. They found that the resting "glow," due to injection of aequorin into a squid axon, was just maintained at the normal intensity when a Ca-EGTA† buffer with an ionized Ca^{2+} concentration of about 3×10^{-7} M (pCa = 6.5) was injected into the axon.

Since the squid axon is not totally impermeable to Ca, even at rest (2; and cf 1, 6), the aforementioned observations all indicate that the squid axon must be able to extrude Ca against about a 60 mV voltage gradient and a 10^4-fold concentration gradient (since $[Ca^{2+}]_o$ in squid blood is about $3–4 \times 10^{-3}$ M; cf 1) in order to remain in steady Ca balance. Obviously, energy is required to power Ca extrusion against this very large electrochemical gradient. In 1969, Blaustein and Hodgkin (3) suggested that at least some of this energy might be derived from the sodium electrochemical gradient. This view was based on the observation that the Ca efflux from ^{45}Ca-injected squid axons was, in part, dependent upon external Na – a requirement which was taken as evidence for Na-Ca coupled counter-transport. Presumably, the energy derived from the inward, "downhill" movement of Na could then be used to move Ca up its electrochemical gradient. The stoichiometry of this counter-transport mechanism could not be determined from the available data, although it was readily apparent that an electrically neutral exchange of $2\ Na^+$–for–$1\ Ca^{2+}$ would not provide sufficient energy to maintain the observed $[Ca^{2+}]_o/[Ca^{2+}]_i$ ratio of about 10^4. However, it was also observed (3) that in cyanide-poisoned axons the magnitude of the Na_o-dependent Ca efflux was not decreased, but was in fact significantly increased. The increased Ca efflux (also cf 7) could be accounted for by an increase in $[Ca^{2+}]_i$ due to release of Ca from axoplasmic sequestration sites such as mitochondria. Cyanide poisoning reduces the axoplasmic ATP concentration about 50-fold, to about 0.1 mM (8), a level sufficiently low to markedly inhibit the axolemmal sodium pumps as indicated by reduction of K_o-dependent and ouabain-sensitive Na efflux (e.g., 9). However, since this reduction of ATP concentration does not inhibit Na_o-dependent Ca efflux, we are left with a dilemma regarding the immediate source of energy for Ca transport. These observations suggest that ATP may not be required for Na-Ca exchange, but they do not provide information about the source of the remainder of the energy required for maintenance of the transmembrane Ca gradient.

§pCa is the negative logarithm of the intracellular ionized Ca^{2+} concentration.

†EGTA = ethylene glycol bis (β-aminoethyl ether) N, N′ tetraacetate.

The present experiments on internally dialyzed squid axons were undertaken in an attempt to resolve this problem. Although a complete solution is not yet available, the new data indicate that Na-Ca exchange may not be electrically neutral, and may indeed be able to derive sufficient energy from the Na electrochemical gradient to maintain a $[Ca^{2+}]_o/[Ca^{2+}]_i$ ratio of about 10^4. These results do not, however, rule out a possible role for ATP in the transport of Ca across the squid axon membrane.

METHODS

Squid Axons

The first stellate nerve was obtained from large, live specimens of Loligo pealei (Woods Hole, Mass.) and from medium-sized live specimens or refrigerated mantles (cf 9) of Loligo forbesi (Plymouth, England). Isolated, cleaned giant axon segments, (4.5 to 5 cm in length, and 500 to 800 μ in diameter) were prepared by standard dissection procedures.

Internal Dialysis Techniques

The axons were cannulated at both ends, onto thin-walled glass end-cannulae which had been mounted in a chamber (see Fig. 1) very similar in design to the one employed by Brinley and Mullins (10). Nearly all of the experimental procedures closely followed the original description of the internal dialysis technique (10). The one major exception was the use of hollow cellulose acetate fibers, rather than porous glass capillaries, to dialyze the axoplasm. The hollow cellulose acetate fibers (195 μ outside diameter and 145 μ inside diameter) were generously given to us by Dr. F. J. Brinley, Jr., or were purchased from Fabric Research Laboratories, Inc. (Dedham, Mass.). Use of these fibers for control of internal solute concentration has already been described by Brinley and Mullins (11). Hollow cellulose acetate fibers are nonporous, and the region which was to be centered within the squid axon had to be rendered porous by hydrolysing the wall to cellulose. This was accomplished by soaking the selected 1.8 cm long section for 16–20 hours in 0.1 N NaOH. When internal dialysis solution (see Table II) containing ^{45}Ca (and 1 mM total Ca) was perfused through the hollow fiber at a rate of 1.1 μl/min, and the fiber was immersed in NaSW (Table I), the rate coefficient for efflux of isotope from the porous region was 0.038 sec^{-1} (that is, nearly 4% of the isotope was lost per second). The diffusion coefficient for Ca through the porous wall was about 0.4×10^{-6} cm^2 sec^{-1}, which is a little less than the value of 1×10^{-6} cm^2 sec^{-1} (for both Ca and CaEGTA) obtained by Brinley and Mullins (11). These diffusion coefficients are about an order of magnitude smaller than the diffusion coefficient for free Ca^{2+} in axoplasm ($2–6 \times 10^{-6}$ $cm^2 sec^{-1}$; 3). Nevertheless, these diffusion parameters (for the hollow fiber and the axoplasm) lead to the prediction that the ^{45}Ca efflux from the axon should reach a steady value with a time constant of about 10–20 min for a 600 μ diameter axon. The experimentally observed time constants were generally of the order of 35 to 40 min.

Hollow cellulose acetate fibers are very flexible, and had to be stiffened with a 100 μ axial wire (either tungsten, purchased from the Rembar Co., Dobbs Ferry, N.Y., or

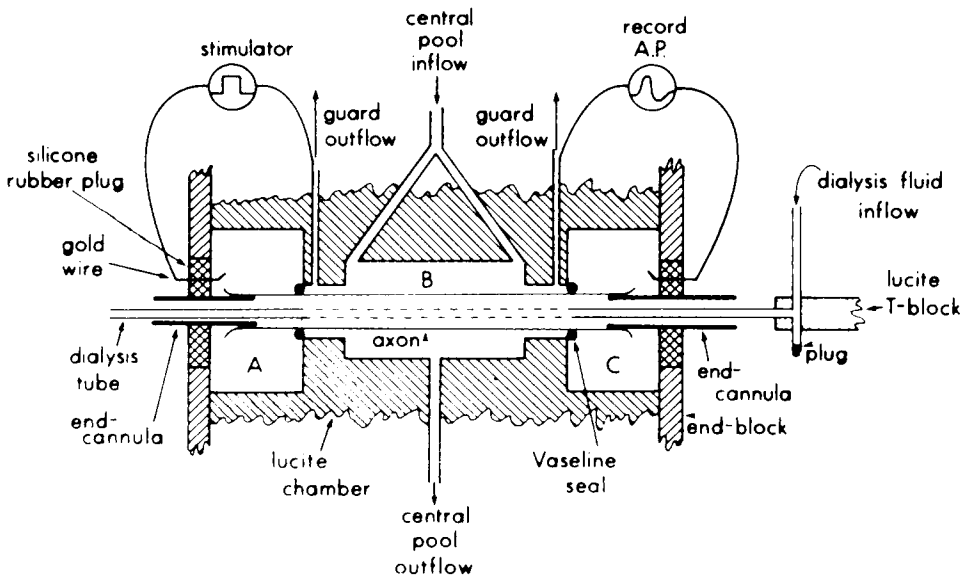

Fig. 1. Diagrammatic view of the experimental apparatus. The view represents a cross section through the experimental chamber, parallel to the upper surface. It is not drawn to scale and is meant primarily to illustrate the relative positions of the axon, hollow cellulose acetate fiber, chamber compartments, and electrodes. The calomel electrodes used to measure membrane potential (see text) have been omitted from the figure; the reference electrode was in contact with the central pool inflow and the "intracellular" electrode was connected to the open left-hand end of the dialysis tube via a salt bridge. The narrow regions of the chamber between compartment B and compartments A and C are the "guard" regions, i.e., the regions surrounding the lateral reaches of the dialyzed protion of the axon. About 3% (or 0.04 ml/min) of the fluid entering the central pool superfused these portions of the axon and then exited through the guard outflows. Only the fluid leaving via the central pool outflow (1.4 ml/min) was sampled for ^{45}Ca activity. Brinley and Mullins (10) should be consulted for details of chamber design.

TABLE I. External Solutions

	Woods Hole Sea Waters*				Plymouth Sea Waters		
	NaSW	Ca-Free NaSW	Ca-Free LiSW	Ca-Free 100 mM KSW	NaSW	Ca-Free NaSW	Choline SW
NaCl	425†	425	0	335	460	460	0
KCl	10	10	10	100	10	10	10
$CaCl_2$	10	0	0	0	11	0	11
$MgCl_2$	25	35	35	35	55	66	55
$MgSO_4$	25	25	25	25	0	0	0
EDTA**	0.1	0.1	0.1	0.1	0	0	0
HEPES§	5	5	5	5	0	0	0
$NaHCO_3$	0	0	0	0	2.5	2.5	2.5
LiCl	0	0	425	0	0	0	0
Choline Cl	0	0	0	0	0	0	460
NaCN	2	2	2	2	2	2	2

*All the Woods Hole solutions were titrated to pH 7.9 at 20°C with Tris base.

**EDTA = ethylene diamine N,N' -tetraacetic acid.

§HEPES = N-2-hydroxyethyl piperazine–N'-2-ethanesulfonic Acid.

†All measurements in mmoles/liter.

boron fiber, generously donated by Mr. D. K. Kuehl of the Hamilton-Standard Company, Windsor Locks, Conn.). With the wire in place, the cellulose acetate fiber could, under direct visual guidance, be readily inserted down the center of the squid axon. The porous region of the cellulose acetate fiber was positioned to lie with one end in each of the "guard" regions (Fig. 1, and cf 10) adjacent to the 1.3 cm wide central compartment (B of Fig. 1) of the chamber, from which external perfusion solution was collected. Thus, the internally dialyzed region of the axon extended about 2.5 mm to either side of the region used for flux measurements.

During the process of cannulation and insertion of the hollow fiber, manipulations which lasted about 20–30 min, the chamber was filled with Ca-free NaSW (Table I) to minimize deterioration of the cut ends of the axon. This fluid contained 2 mM NaCN to initiate reduction of the axoplasmic ATP concentration.

With the cellulose acetate fiber in place, and the axon properly positioned in the chamber, the end pools (A and C of Fig. 1) could be sealed off (cf 10). The internal and external fluid flows were turned on, and the stiffening wire was carefully withdrawn from the open distal end of the hollow fiber [the other end of the hollow fiber was sealed in a lucite T-block (Fig. 1)]. The fluid superfusing the central (dialyzed) region of the axon was then switched to standard NaSW (containing Ca and 2 mM CN; Table I).

The position of the porous region of the cellulose acetate fiber could be confirmed after a few minutes of dialysis because all internal solutions contained 0.5 mM phenol red, which rapidly dyed the dialyzed region of axoplasm a bright red. Routinely, axons were dialyzed with unlabeled internal solution for 15–20 min before ^{45}Ca was introduced. During this period a salt bridge was set up for membrane potential recording (see below) and the resting potential was measured to ascertain the stability of the preparation. Action potentials, conducted through the dialyzed region of the axon, were also monitored.

Electrical Recording

The open distal end of the hollow cellulose acetate fiber was connected, via a 3 M KCl bridge, to a calomel electrode for measurement of the axon resting potential. The reference electrode, also a calomel cell, was fixed in the inflow line (Fig. 1) of the fluid which superfused the central dialyzed region of the axon. The potential difference between these electrodes was either read directly off the meter of a Keithley 610C electrometer (at Woods Hole) or fed through a Transidyne General MPA2 preamplifier to a strip chart recorder (at Plymouth).

A gold wire electrode was fixed in the silicone rubber seal of each end block, adjacent to the end cannula (see Fig. 1). One, connected to a Grass SD–9 stimulator, was used to pass current. The evoked action potential, after conduction through the dialyzed section of the axon, was recorded through the other gold wire electrode and monitored on a Tektronix 502A oscilloscope. Ground leads for the stimulator and oscilloscope were connected to the chamber through the guard fluid outflows (see Fig. 1). Vaseline seals surrounded the axon in the guard regions and separated the guard regions from the end pools (see Fig. 1); this increased the extra-axonal resistance between the guard and the end-pool regions.

Normally, the cyanide-poisoned (ATP-depleted) dialyzed axons continued to conduct action potentials in NaSW for several hours. However, after an hour or more of ex-

posure to cyanide, switching to Ca-free sea water rendered the axons irreversibly inexcitable, despite maintenance of the resting potential. In general, a spontaneous depolarization of the membrane to about −40 to −45 mV signaled the end of an experiment, as the external Na- and Ca-independent Ca efflux began to rise at an appreciable rate.

Solutions

The composition of representative external (artificial sea water) solutions are given in Table I. In all the Ca-free or Ca-depleted solutions, $CaCl_2$ was replaced by an isosmolar amount of $MgCl_2$. In some instances, mixtures of two solutions (e.g., Ca-free NaSW and Ca-free LiSW) were used in order to obtain the desired Na or Li concentrations (see Results). In some instances veratridine (from ICN-K & K Laboratories, Inc., Plainview, New York) and/or tetrodotoxin (from Calbiochem, La Jolla, Calif.) were added to the external medium; details will be given in the Results section.

TABLE II. Internal (Dialysis) Fluids

	Woods Hole*	Plymouth*
K isethionate	350**	0
K glutamate	0	400
Na isethionate	50	50
$MgCl_2$	10	10
Tris-HEPES, pH 7.0	5	5
Taurine	200	200
Phenol red	0.5	0.5
KCN	2	2

*Information about the addition of $CaCl_2$ and EGTA to these solutions will be given in the Results section.

**All measurements in mmoles/liter.

Table II shows the composition of the standard internal (dialysis) fluids. The concentration of Ca and of EGTA in these fluids varied from experiment to experiment, and will be mentioned when the results of the individual experiments are described. In all experiments, the amount of Ca in the nonradioactive solutions was determined by atomic absorption spectroscopy; the Ca concentration of the $^{45}CaCl_2$ solution used at Woods Hole was assayed by the calcein fluorescence technique (12). The concentration of ionized Ca^{2+} in the Ca-EGTA buffers (given in the figure legends) was calculated on the basis of a CaEGTA association constant of $7.6 \times 10^6\ M^{-1}$ (13).

An unfortunate feature of the Woods Hole experiments was the fact that the taurine (from Eastman Kodak Co., Rochester, N.Y.) was severely contaminated with Ca. This accounts for the low pCa in these experiments. Under these conditions, nearly all of the Ca efflux was Na_0- and Ca_0-dependent (e.g., Fig. 2). Subsequent experiments, with higher pCa's (at Plymouth), gave qualitatively similar results (e.g., compare Figs. 6 and 8), although a smaller fraction of the total Ca efflux was dependent upon external Na and Ca.

In those experiments in which the effect of the internal Na concentration on Ca efflux was tested, the sum of the Na isethionate and K isethionate concentrations was maintained constant, while the ratio of the two was varied to give the desired $[Na^+]_i$.

In a few experiments, as noted in the appropriate figure legends, oligomycin (Sigma Chemical Co., St. Louis, Mo.), dissolved in ethanol, was added to the dialysis fluid. The magnitude and cation dependence of the Ca efflux was unaffected by either the ethanol (0.2 vol%) or the oligomycin (125 μgm/ml). When used, ATP was added as the dipotassium salt (Sigma Chemical Co., St. Louis, Mo.).

Radioactive Tracer Techniques

The ^{45}Ca (as $^{45}CaCl_2$ from New England Nuclear, Boston, Mass.) concentration in dialysis fluid was usually about 25 μCi per ml. All ^{45}Ca activities were assayed by liquid scintillation spectroscopy. At Woods Hole, 2.2 ml of external solution, or a 2.2 ml aliquot of dialysis fluid diluted in NaSW, was added to 15 ml of dioxane-based scintillation cocktail (8 gm "Omnifluor," from New England Nuclear, Boston, Mass.; 60 gm naphthalene; 20 ml ethylene glycol; 100 ml methanol; diluted to 1 liter with 1, 4-dioxane). At Plymouth, 2.0 ml of solution was added to 10 ml of toluene-Triton X-100 scintillation cocktail (4 gm PPO; 0.2 gm POPOP; 333 ml Triton X-100; and 667 ml toluene).

RESULTS

Effect of External Na Concentration

Figure 2 shows the data from a representative experiment in which the effect of the external Na concentration ($[Na]_o$) on Ca efflux was determined. The main observation is that in axons with a rather high $[Ca^{2+}]_i$ (pCa = 3.5–3.7), nearly all of Ca efflux into Ca-free sea water (indicated by the open circles) is Na_o-dependent. As noted in the Introduction, this finding may be evidence that Ca extrusion involves an exchange of Ca for Na.

The data of Fig. 2 also provide some information about the interrelationship be-between $[Na]_o$ and Ca efflux: Ca efflux is minimally increased when $[Na]_o$ is raised from 2 mM to 44 mM; but the Ca efflux into a solution containing 129 mM Na is about 70% of the efflux into the standard Ca-free NaSW (containing 426 mM Na). These data indicate that the relationship between $[Na]_o$ and Ca efflux is sigmoid, with a very flat foot near the origin, and a steeply sloping region. Further evidence for this type of relationship is given in Fig. 3, which shows the averaged data from five axons. The sigmoid curve may indicate that more than one Na^+ ion is required to activate the efflux of each Ca^{2+} ion. The solid line in the figure has been calculated on the assumption that the cooperative action of two Na^+ ions is required, while the broken line fits a cubic relationship between $[Na]_o$ and Ca efflux (see legend to Fig. 3). The fact that the broken line gives a better fit to the data, particularly at the low $[Na]_o$ end of the curve, suggests that the cooperative action of three Na^+ ions may be required to activate the efflux of one Ca^{2+}. One possibility which might provide this type of kinetic interrelationship is a coupled exchange of three Na^+ for one Ca^{2+}.

The Effect of Membrane Potential on Ca Efflux

The aforementioned coupled transport, involving an unequal movement of charge

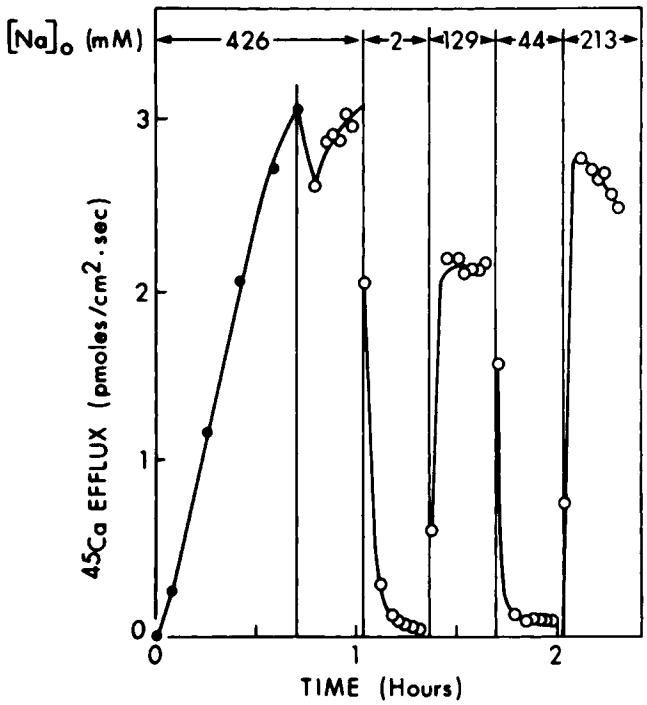

Fig. 2. Effect of external Na on Ca efflux. Internal dialysis with ^{45}Ca-containing solution was begun immediately after the first (background) point was obtained. Solid circles refer to Ca-containing seawater; open circles refer to Ca-free SW. The numbers at the top refer to the Na concentration in the external medium; Na was replaced isosmotically by Li in the Na-depleted solutions. Loligo pealei axon 05213. Diameter = 6.30 μ, $[Ca]_T$ = 215 μM, $[EGTA]_T$ = 15 μM, pCa = 3.7. Membrane potential = 58 mV. Temperature = 15°C.

in opposite directions across the membrane, might be expected to be directly influenced by the transmembrane voltage gradient. Indeed, Brinley and Mullins (11) have observed that depolarization inhibits Na_0-dependent Ca efflux from dialyzed squid axons. The data in Fig. 4, taken from one of our experiments, confirms their finding. In this experiment the axon was first depolarized with 1.5×10^{-4} M veratridine (14), and repolarized with 10^{-6} M tetrodotoxin (14). A subsequent brief exposure to Ca-free 100 mM K sea water also induced a reversible depolarization. Both depolarizations were associated with partially reversible declines in Ca efflux. This is particularly striking because depolarization (i.e., an increase in intracellular positivity) might have been expected to increase rather than decrease the efflux of a cation. However, this behavior could be accounted for if the efflux of Ca was accompanied by net entry of positive charge, as required by the 3:1 Na–Ca exchange model.

A graph of the logarithm of the Ca efflux vs. membrane potential is shown in Fig. 5, which contains data from 8 axons. The Na_0-dependent Ca efflux (M_0^{Ca}) should be related to the membrane potential (V) by an expression of the form:

$$M_0^{Ca} \propto \exp \frac{-VFZ}{RT}$$

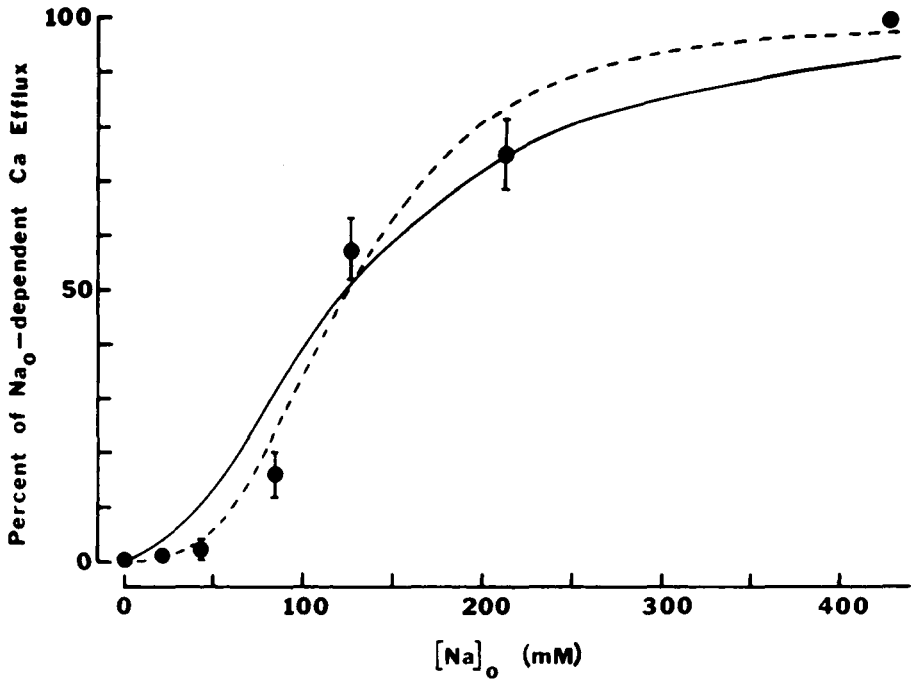

Fig. 3. Percent of maximal Na_0-dependent ^{45}Ca efflux from internally dialyzed squid (Loligo pealei) axons graphed as a function of the external Na concentration. The data are mean values from five axons, including the axon of Fig. 2; the standard errors are indicated by the vertical bars. The axons were internally dialyzed with an ATP-free solution containing 2 mM cyanide; the pCa was 3.5–3.7; the temperature was 15 ± 1°C. The Na_0-dependent Ca efflux into Ca-free NaSW, taken as 100% in the graph, averaged 3.85 ± 0.25 pmoles $cm^{-2}sec^{-1}$; the mean efflux into Ca-free Na-free sea water was 0.07 ± 0.01 pmoles $cm^{-2}sec^{-1}$. Lithium was substituted isosmotically for Na in all of these experiments. The smooth curves fit the equation

$$v = \frac{V}{\left(1 + \frac{\bar{K}_{Na}}{[Na]_o}\right)^n}$$

where v is the Na_0 -dependent ^{45}Ca efflux at any external Na concentration ($[Na]_o$), relative to that in Ca-free NaSW (V); $\bar{K}_{Na}$ is the apparent half-saturation constant for Na_0, with a value of 125 mM. The exponent, n, had a value of 2 (solid line) or 3 (dashed line).

where F, R, and T are Faraday's number, the gas constant and absolute temperature, respectively, and Z is the net inward charge movement associated with the efflux of one Ca^{2+} ion. The broken line in the figure has a slope equivalent to an e-fold (2.7-fold) reduction in Ca efflux for a 25 mV depolarization; i.e., it gives the slope expected if the exit of each Ca^{2+} ion is accompanied by the net entry of one positive charge (or the net exit of one negative change). The experimental data shown in the figure are all consistent with a value for $Z \leqslant 1+$. If all of the observed Ca efflux is not Na_0-dependent, the apparent value of Z would be reduced; consequently, some of the smaller values of Z might

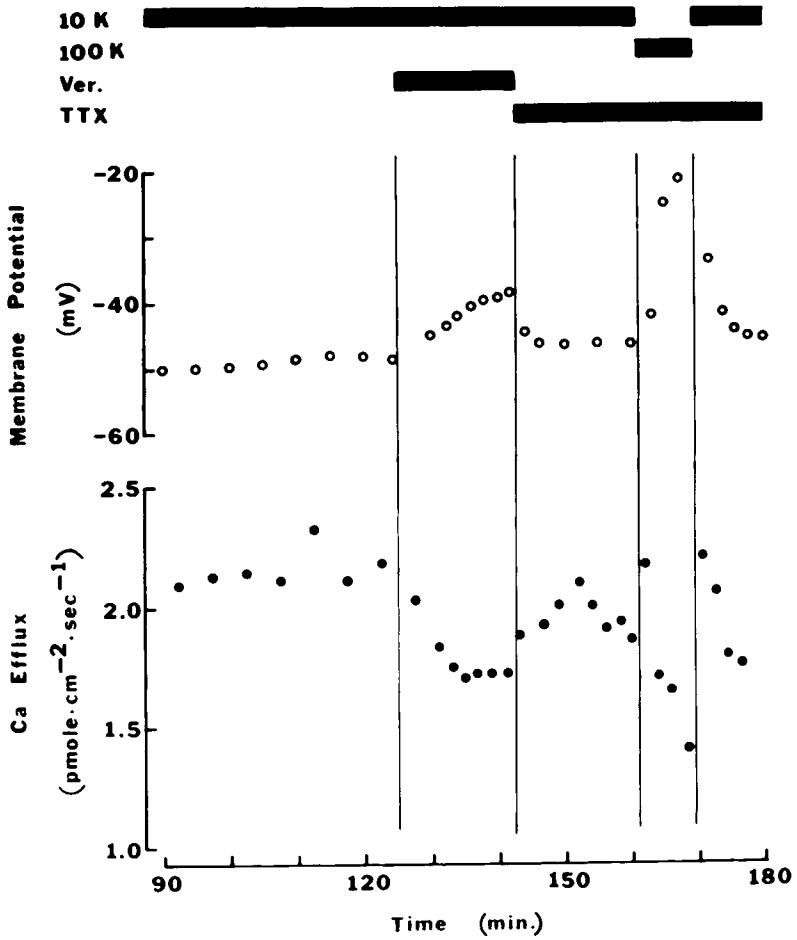

Fig. 4. Effect of membrane potential on ^{45}Ca efflux (solid circles, lower portion of figure) from an internally dialyzed squid axon. The time indicated on the abscissa refers to the elapsed time from the start of the internal dialysis. The membrane potential, recorded from the distal end of the dialysis tube, is shown in the middle part of the figure. The bars at the top indicate the presence in the external medium of either 10 mM K (10K) or 100 mM K (100K), and of 5×10^{-4} M veratridine (Ver) or 10^{-6} M tetrodotoxin (TTX). The veratridine and K-rich solutions were used to depolarize the axon; TTX is known to reverse veratridine-induced depolarization in squid axons (14). Loligo pealei axon 6013b; diameter 630 μ; temperature = 15°C. The internal dialysis fluid had a pCa of 3.7.

simply be the result of neglecting a relatively large Na_0 -independent component of Ca efflux (unfortunately, the Na_0 -dependence of the Ca efflux could not always be tested before terminating these experiments).

Ca-Ca Exchange: The Influence of External Cations

Ca efflux is also influenced by the external Ca concentration ($[Ca]_0$). The effect is clearly seen in Fig. 11, where the Ca efflux declined by about 15% when external Ca was

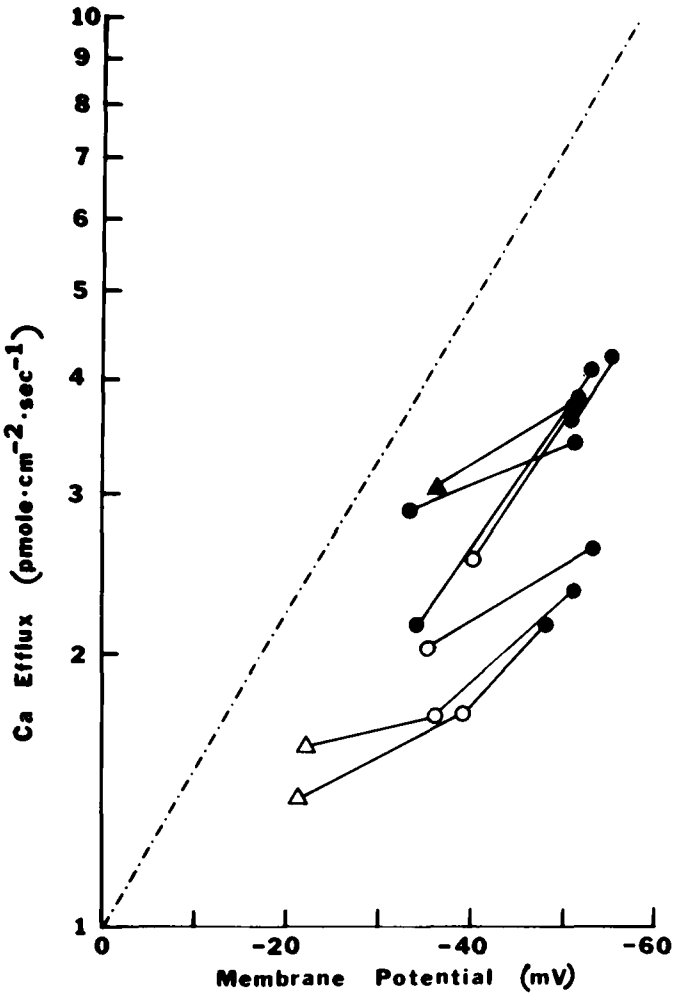

Fig. 5. Effect of membrane potential on ^{45}Ca efflux from internally dialyzed squid axons. Data from eight Loligo pealei axons (including the axon of Fig. 4) are summarized in the figure; data from individual axons are connected by solid lines. ^{45}Ca efflux into Ca-free sea water containing 10 mM K and 425 mM Na is indicated by solid circles. In some instances the axons depolarized spontaneously, as denoted by two solid circles connected by a line. In other instances 50 mM K (▲) or 100 mM K (△) or 5×10^{-4} M veratridine (○) was used to depolarize the axons. All axons were dialyzed with ATP-free solution containing 2 mM cyanide; the pCA was 3.5–3.7, and the temperature was 15 ± 1°C. The broken line (– · – · –) has a slope equivalent to an e-fold reduction in Ca efflux for a 25 mV depolarization.

replaced by Mg after the ^{45}Ca efflux into standard NaSW had reached a steady level. (In experiments such as those of Figs. 2 and 6, where external Ca was removed before a steady efflux was attained, the replacement of external Ca caused a transient decline in the rate of rise of the ^{45}Ca efflux.) External Ca-dependent Ca efflux, which has also been observed in unpoisoned and in cyanide-poisoned intact (as opposed to "dialyzed") squid

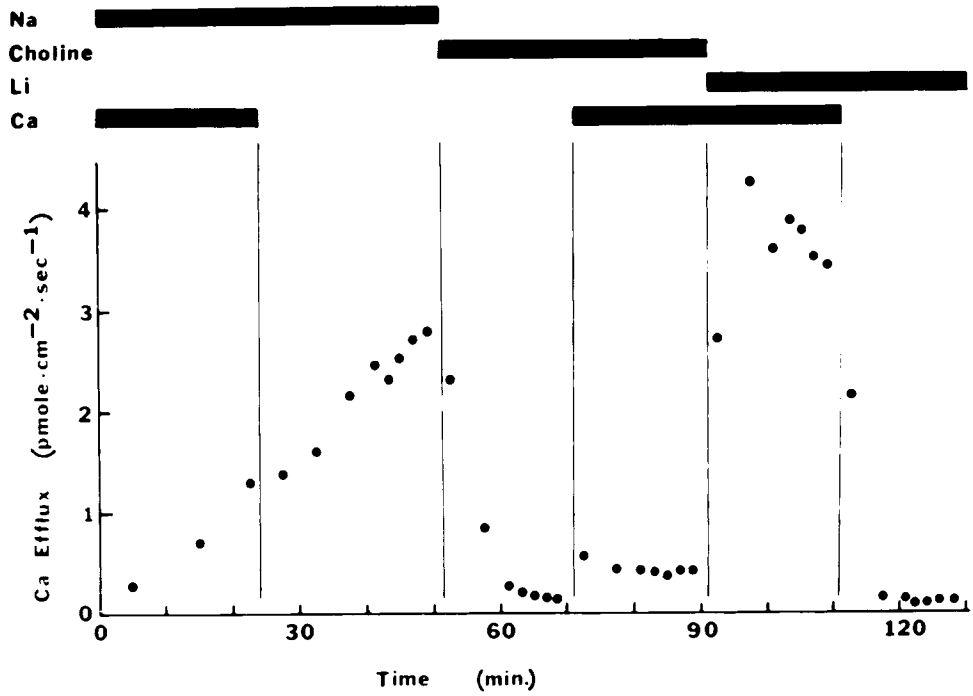

Fig. 6. Effect of external cations on the ^{45}Ca efflux from an internally dialyzed squid axon. The bars at the top of the figure indicate the presence of the appropriate cations. The Ca concentration in the Ca-containing solutions was 10 mM; Ca was replaced by Mg in Ca-free solutions. The concentrations of Na, Li, and choline were 425 mM. The dialysis solution had a pCa of 3.3. Loligo pealei axon 06033. Diameter = 560 μ. Membrane potential = −56 mV. Temperature = 15°C.

axons (3), may be indicative of a Ca-Ca "exchange diffusion" process (cf 15).

The foregoing evidence for an apparently unequal charge exchange involved in the Na_0-independent Ca efflux (presumably Na-Ca exchange) led us to examine the influence of other cations on the Ca_0-dependent Ca efflux. The main result is illustrated in Fig. 6. which shows that the Ca efflux is dramatically reduced when external Na is replaced by choline in the absence of external Ca. Only a small increase in Ca efflux resulted when Ca was added to the choline SW, but replacement of the choline by Li markedly stimulated Ca efflux. That the Ca efflux into LiSW is Ca_0-dependent is demonstrated by its prompt decline upon removal of external Ca. These observations have recently been confirmed on intact ^{45}Ca-injected squid axons by P. F. Baker (personal communication).

The idea that the foregoing observations are manifestations of a Ca-Ca exchange mechanism in squid axons is supported by data from Ca influx studies. Baker et al. (9) have shown that Ca influx is increased when external Na is reduced; but, whereas Ca influx increases monotonically when Na_0 is replaced by Li, replacement by dextrose causes Ca influx to peak at an $[Na]_0$ of about 100 mM, and to decline upon further reduction of $[Na]_0$ (Fig. 7A). These data suggest that the Ca influx is obligatorily accompanied by the inward movement of an alkali metal ion (Li or Na). Presumably, during Ca-Ca exchange, the Ca transport mechanism has two types of sites which are

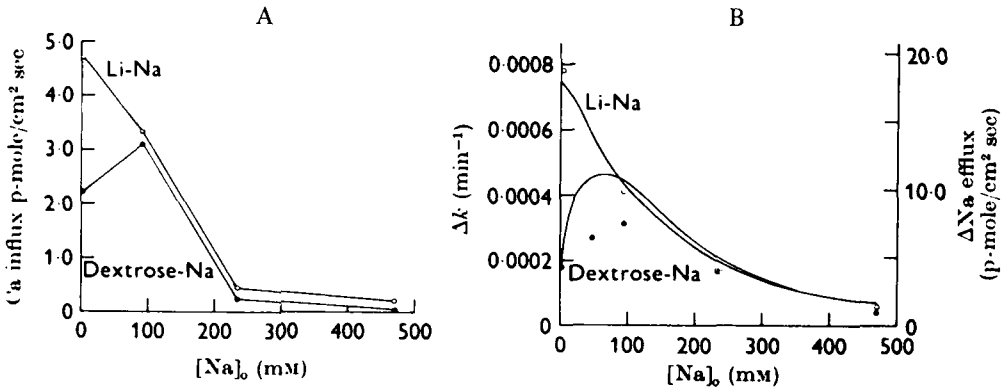

Fig. 7 (A). Effect of external sodium concentration on calcium influx in Loligo forbesi axons using Li, upper curve (○), or dextrose, lower curve (●), as a replacement for Na. Averaged results obtained on 14 axons from 7 squid (Li), and 16 axons from 8 squid (dextrose). Abscissa: Na concentration in mM. Ordinate: Ca influx. K-free solutions containing 10^{-5} M ouabain were used. (B) Effect of replacing external Na by Li or dextrose on Ca_0-dependent Na efflux from Loligo forbesi axons in the presence of 10^{-5} M ouabain. (○) Average Ca_0-dependent Na efflux for Li-Na mixtures (three experiments). (●) Average Ca_0-dependent sodium efflux for Na-dextrose mixtures (two experiments) in which the efflux in LiSW was also determined. The mean increment on replacing Na by Li (in the presence of Ca) in these two experiments was the same as in the three experiments from which the Li-Na curve was obtained. Ordinate: left-hand scale, fraction of ^{22}Na lost per minute; right-hand scale, the sodium efflux (in pmole $cm^{-2}sec^{-1}$) based on an average diameter for these 5 axons of 822 μ, and a mean intracellular sodium concentration for all refrigerated mantle axons tested of 70 mM/kg axoplasm. The smooth curves were drawn to fit a model described in the orginal text (from Baker et al., 9).

(perhaps simultaneously) exposed to the external medium: one type binds Ca while the second type is occupied by an alkali metal ion (Na or Li) but not by choline.

In order to characterize further the Ca transport mechanism, the apparent dissociation constants for external Ca and Li were determined. Figure 8 presents data from an experiment in which Ca efflux was measured in mixtures of Li and choline sea waters. The results are graphed as a function of $[Li]_0$ in Fig. 9. The Ca efflux appears to saturate at high $[Li]_0$; although the data do not give a very good fit to the rectangular hyperbola, they do indicate that the Li_0-dependent Ca efflux is half-maximal at an $[Li]_0$ of about 100 mM.

The Ca efflux into LiSW was also measured as a function of $[Ca]_0$, and the data were fitted to a rectangular hyperbola. As shown in Fig. 10, the Ca efflux is half-maximal at a $[Ca]_0$ of about 3 mM. However, if Mg is a weak inhibitor of the Ca efflux (or can serve as a partial substitute for external Ca; cf Ref. 3), the value of 3 mM for K_{Ca} may be an overestimate.

Inhibition of Ca Efflux by Internal Na

Ca entry into squid axons is promoted by increasing $[Na]_i$ and/or lowering $[Na]_0$,

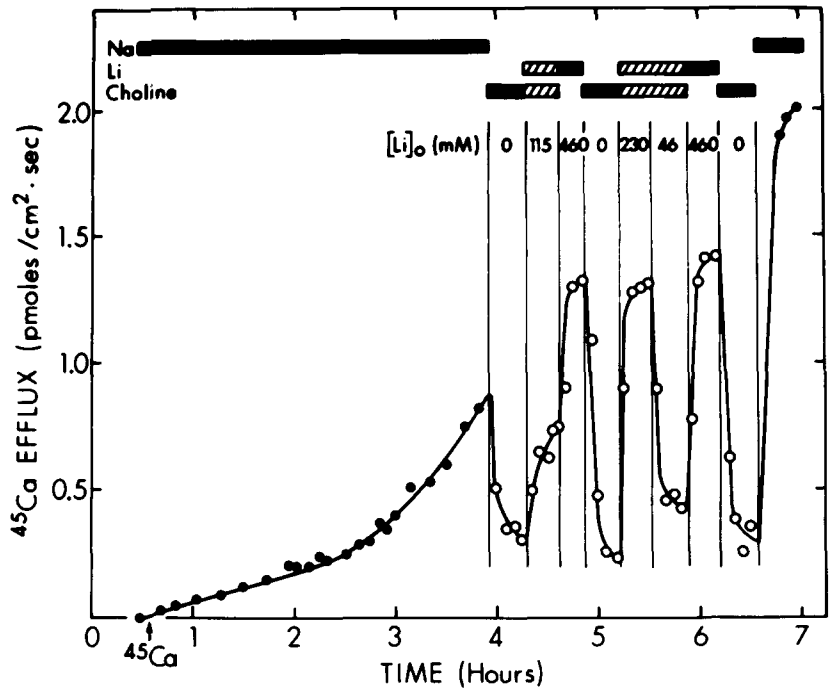

Fig. 8. Effect of mixtures of LiSW and choline SW on Ca efflux. The internal dialysis with ^{45}Ca-containing solution was begun at the time indicated by the arrow. The presence of Na, Li, or choline in the external medium is indicated by the bars at the top of the figure; all solutions contained 11 mM Ca. When mixtures of Li and choline were used (indicated by the hatched bars), the sum of Li + choline was always 460 mM; the Li concentrations are shown on the figure. Loligo forbesi axon 12063. Diameter = 670 μ, $[Ca]_T$= 1.1 mM, $[EGTA]_T$ = 1.3 mM, pCA = 5.9. Resting potential = −64 mV. Temperature = 15°C. The dialysis fluid for this experiment contained 125 μgm oligomycin per ml.

and external Na appears to compete with Ca at the Ca entry sites (9). Since Ca efflux is, in part, dependent upon external Na, it seemed logical to determine whether or not the internal Na concentration also influences Ca efflux. The data in Fig. 11 show that lowering $[Na]_i$ from 50 to 25 mM increased Ca efflux, while raising $[Na]_i$ to 100 mM reduced Ca efflux. The relationship between $[Na]_i$ and Ca efflux is shown graphically in Fig. 12; the data from the experiment of Fig. 11 and seven similar experiments are included. Although the curve does indicate that internal Na inhibits Ca efflux, it is not as steep as expected if, for example, two Na^+ ions compete with one Ca^{2+}. However, even with a 2-to-1 competition, the observed curve might be accounted for if the relatively high $[Ca^{2+}]_i$ (200–500 μM) present in these experiments was sufficient to saturate the internal site of the Na-Ca exchange mechanism (see Discussion).

The Effect of ATP on Ca Efflux

All of the experiments described in the preceding sections have been carried out on ATP-depleted axons; i.e., on axons which were poisoned with cyanide and dialyzed with

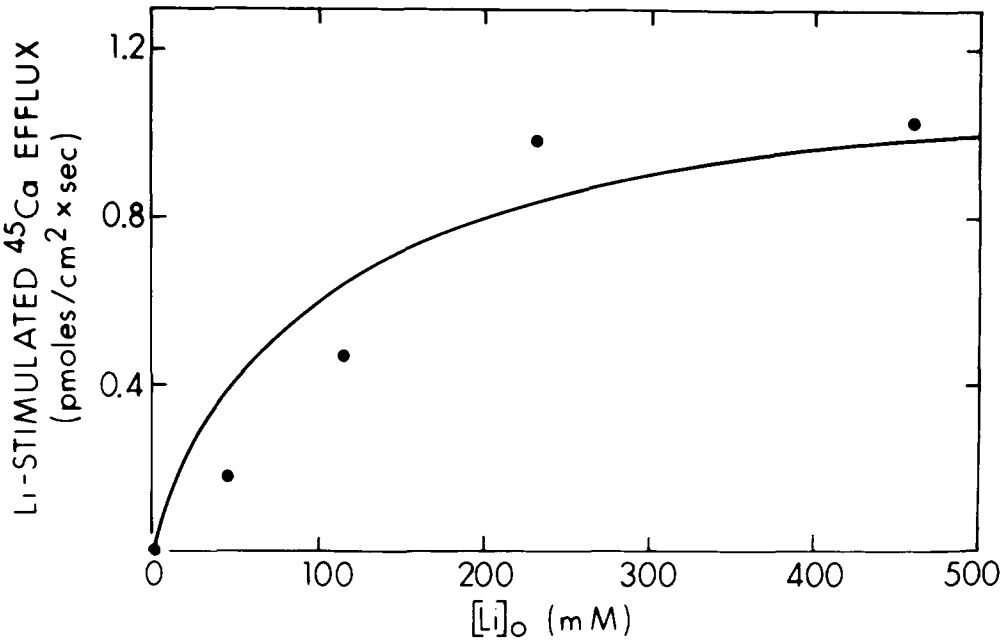

Fig. 9. Li_0-stimulated Ca efflux graphed as a function of the external Li concentration ($[Li]_0$). The data for the effluxes into LiSW-choline SW mixtures from the experiment of Fig. 8 were used here. The theoretical curve fits the equation

$$v = \frac{V}{1 + \frac{K_{Li}}{[Li]_o}}$$

where v is the Li_0-stimulated Ca efflux at any $[Li]_0$ and V is the maximal Li_0-stimulated Ca efflux with a value of 1.2 pmoles cm^{-2} sec^{-1}. The apparent dissociation constant for Li, K_{Li} has a value of 100 mM.

ATP-free solutions. Cyanide poisoning alone is known to reduce axoplasmic ATP levels to about 100 μM (8). Although ATP levels were not measured, they must have been considerably lower than 100 μM after several hours of dialysis. In view of the maintained Na_0-dependent Ca efflux under these conditions, which are sufficient to curtail markedly ATP-dependent Na extrusion (16–18), it seems reasonable to conclude that Na-Ca exchange does not have an absolute requirement for ATP. Nevertheless, Baker and Glitsch's (19) evidence that axoplasmic ATP levels may influence the kinetics of Na_0-dependent Ca efflux makes it imperative that the effect of ATP on Ca efflux be subjected to close scrutiny. Figure 13 shows data from a preliminary experiment in which the effect of ATP was tested on Ca efflux into Na-containing and Na-free (choline) sea waters. A superficial examination of these data might lead one to suspect that the large increment in Na_0-dependent Ca efflux which was observed following the addition of ATP to the dialysis fluid was, in fact, ATP-dependent. However, comparison of these data with the data of Fig. 8, where ATP was not added to the dialysis fluid, indicates

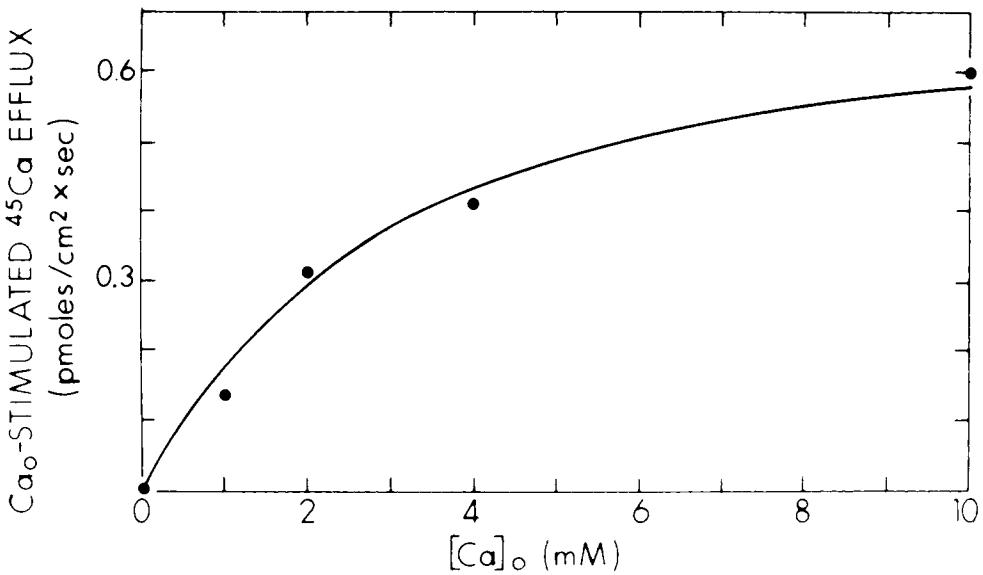

Fig. 10. Ca_0-stimulated Ca efflux into LiSW graphed as a function of $[Ca]_0$. The data are from an experiment similar in design to that of Fig. 8, except that $[Ca]_0$ was varied between 0 and 10 mM, while $[Li]_0$ was maintained at 460 mM. The theoretical curve fits the equation

$$v = \frac{V}{1 + \frac{K_{Ca_0}}{[Ca]_0}}$$

where v is the Ca_0-stimulated Ca efflux at any $[Ca]_0$, and V is the maximal Ca_0-stimulated Ca efflux with a value of 0.75 pmoles cm^{-2} sec^{-1}. The apparent dissociation constant for Ca, K_{Ca_0} has a value of 3 mM. The Ca efflux into Ca-free LiSW was 0.20 pmoles $cm^{-2}sec^{-1}$. Loligo forbesi axon 12113. Diameter = 640 μ. $[Ca]_T$ = 1.1 mM, $[EGTA]_T$ = 1.3 mM, pCA = 5.9. Resting potential = −47 mV. Temperature = 15°C. The dialysis fluid contained 125 μgm oligomycin per ml.

that considerable caution must be exercised in interpreting these results. In the experiment of Fig. 8 a delayed rise of the Ca efflux into NaSW occurred about 3 hours after the start of internal dialysis; most of the increment appears to be Na_0-dependent since the Ca efflux into choline SW remained relatively constant during the period between 4 and 6½ hours. Although the explanation for the delayed appearance of this large Na_0-dependent Ca efflux is unknown, the observations made in the absence (Fig. 8) and in the presence (Fig. 13) of ATP appear comparable. This suggests that the introduction of ATP may not have been the primary factor responsible for the increase in Na_0-dependent Ca efflux seen in Fig. 13. Di Polo (20) has also concluded that the Na_0 + Ca_0-dependent Ca efflux from internally dialyzed squid axons is largely ATP-independent. However, the transient fall in the Ca efflux following removal of ATP (Fig. 13) may indicate that the effect of ATP cannot be ignored entirely. Clearly, additional experimentation will be required to sort out the effects of ATP on Ca efflux.

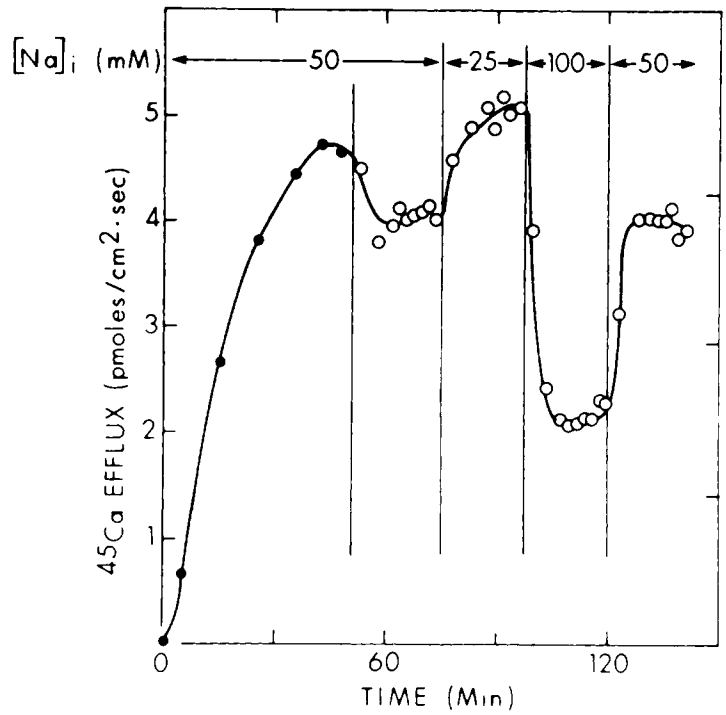

Fig. 11. Effect of $[Na]_i$ on ^{45}Ca efflux into a Ca-free NaSW. In this experiment, the sum of the Na isethionate + K isethionate in the dialysis fluid was maintained constant at 400 mM, while the ratio of the two salts was varied to give the $[Na]_i$ shown in the upper part of the figure. The external medium was either standard NaSW (solid circles) or Ca-free NaSW (open circles). Dialysis with ^{45}Ca-containing fluid was begun immediately after the first (background) point was obtained. Loligo pealei axon 05173a. Diameter = 525 μ. pCa = 3.3. Resting potential = 55 mV. Temperature = 15°C.

DISCUSSION

Evidence for Carrier-Mediated Na-Ca and Ca-Ca Exchange

The present series of experiments has been concerned primarily with the effects of external and internal cations on Ca efflux from dialyzed squid axons. The main point is that Ca efflux is promoted by external Na and inhibited by internal Na; the Ca efflux seems to be a cubic function of $[Na]_0$ and is voltage-sensitive.

Earlier studies on intact axons have shown that Ca efflux is partially Na_0-dependent (3). Furthermore, Ca influx is inhibited by high external Na and stimulated by internal Na (9). There is also evidence for a Ca_0-dependent Na efflux, which operates under the same conditions as does the Na_i-dependent Ca influx (9; and see Fig. 7).

The most straightforward unifying hypothesis which takes all these phenomena into account is the idea of a counter-transport mechanism which can move Ca across the axolemma in exchange for Na. Unfortunately, the picture is still somewhat incomplete,

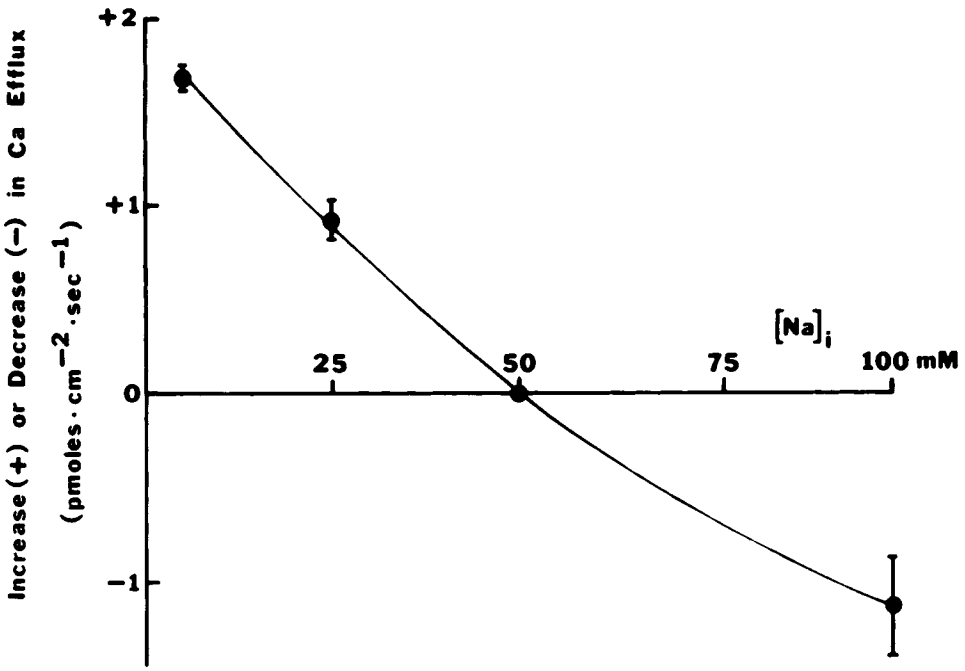

Fig. 12. ^{45}Ca efflux into Ca-free NaSW graphed as a function of $[Na]_i$. The figure shows the increment (+) or decrement (−) in the efflux, relative to the efflux from axons dialyzed with a solution containing 50 mM Na. For this case ($[Na]_i$ = 50 mM), the mean efflux into Ca-free Na-containing sea water was 3.01 ± 0.38 pmoles $cm^{-2}sec^{-1}$. The data are the mean values for 8 Loligo pealei axons including the axon of Fig. 11; the standard errors for the effluxes are indicated by the vertical bars. The dialysis fluids had a pCa of 3.5–3.7. The sum of $[Na]_i$ + $[K]_i$ (present as the isethionates) was always 400 mM. Temperature was 15 ± 1°C.

since an expected corrollary of this model, namely, the existence of a Ca_i-dependent Na influx, has not as yet been demonstrated.

The Ca efflux is also in part dependent upon external Ca, and some of the properties of this efflux, reported here, are rather similar to those of Ca influx in squid axons (9; and see Fig. 7A). Both influx and efflux of Ca are prominent in LiSW and are reduced at high $[Na]_o$ or in media containing very low alkali metal ion concentrations. These phenomena can be most readily explained by a Ca-Ca coupled exchange mechanism.

All these observations, taken together, support the view that in squid axons the Ca efflux mechanism may involve both Na-Ca exchange and Ca-Ca exchange whose relative magnitudes depend upon the prevailing ionic conditions. This type of counter-transport behavior suggests that a mobile carried-mediated process may be involved (21, 22).

A Model for Carrier-Mediated Ca Efflux

In order to account for all of the cation interactions described above, we require a carrier mechanism with two types of sites. One type of site presumably binds either two Na^+ ions or one Ca^{2+} ion, and is responsible for the basic properties of either Na-Ca ex-

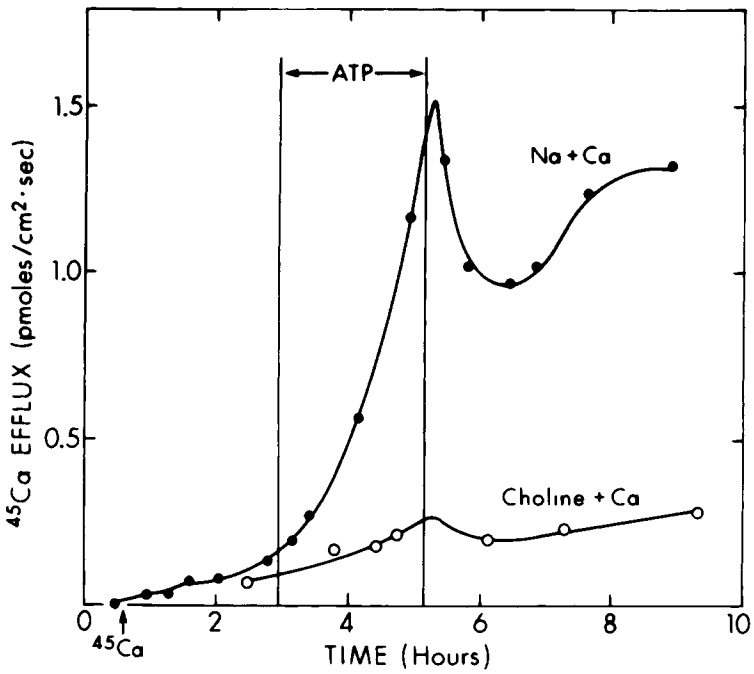

Fig. 13. Effect of ATP on Ca efflux into NaSW and choline SW. Internal dialysis with ^{45}Ca-containing fluid was begun at the time indicated by the arrow. During the entire experiment the dialysis fluid contained 125 μgm oligomycin per ml. During the period indicated, the dialysis fluid also contained 3 mM ATP. Each symbol on the graph indicates the mean Ca efflux determined from 3 or 4 consecutive 2 min samplings of external medium effluent: the solid circles refer to the efflux into NaSW, and the open circles, to efflux into choline SW. Loligo forbesi axon 12183b. Diameter = 650 μ. $[Ca]_T$ = 1.0 mM, $[EGTA]_T$ = 2.0 mM, pCa ≃6.8. Resting potential = −55 mV. Temperature = 16°C.

change or Ca-Ca exchange. It is difficult to envision a single site into which either a Ca^{2+} or two Na^+ ions could fit (so as to account for Na-Ca competition); a somewhat more attractive possibility is that there are two neighboring sites, one for Ca^{2+} and one for 2 Na^+, which are allosterically linked and mutually exclusive. Consequently, occupation of the Na site by one or two Na^+ ions would prevent access of Ca^{2+} to the adjacent site.

In addition, another type of ("activator") site is required to account for such properties as the Li-dependent Ca fluxes, the cubic relation between $[Na]_0$ and Ca efflux, and the voltage sensitivity of the Ca efflux. This (second) site presumably accepts a single small monovalent cation, either Na^+ or Li^+, but not choline. The experimental evidence indicates that this site must be occupied on the inward journey of the carrier.

A scheme which illustrates the behavior of a carrier mechanism of this type is shown in Fig. 14. The free carrier (R) bears a net charge of 3−, 2− at the Na-or-Ca site, and 1^- at the activator site. This carrier could, presumably, move Na or Ca in either direction across the membrane. The long arrows in the figure indicate the preferred movements of the carrier when a small load of Ca is deposited at the inner surface of the membrane: the carrier presumably moves out with a Ca^{2+} and with the activator site (bearing

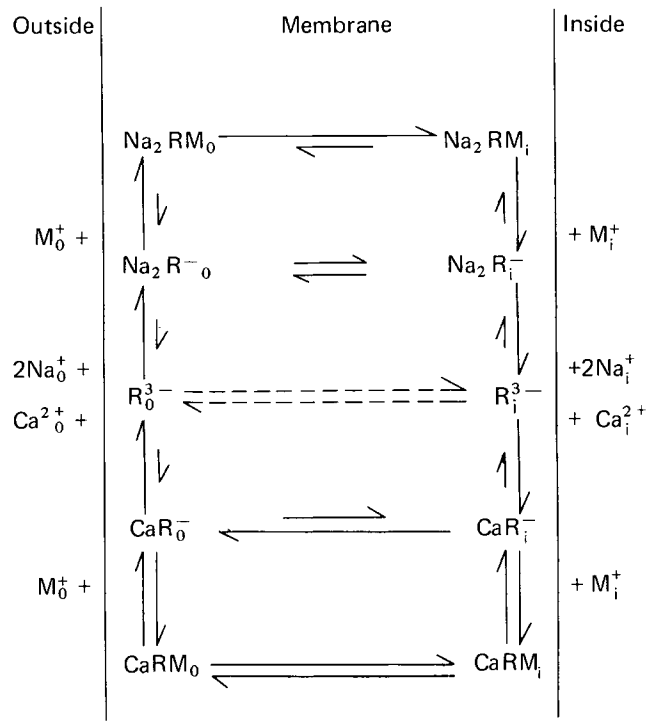

Fig. 14. Model of a sodium-calcium counter-transport carrier mechanism. The free carrier, R^{3-}, is assumed to have two types of cation-binding sites. One site is monovalent and can bind a single alkali metal ion (M^+, either Li^+ or Na^+); the second site is divalent, with specificity for either Na (two Na^+ ions can bind) or Ca. The chemical reactions between carrier and counter ions are assumed to be very rapid, while the diffusion of the carrier complexes across the membrane are rate-limiting. The diffusible carrier-cation complexes are: Na_2RM, $CaRM$, Na_2R^-, and CaR^- (the latter two are driven by the membrane potential and therefore move preferentially in the outward direction). Free carrier (R^{3-}) is assumed to diffuse slowly, if at all. The long solid arrows show the directions the reactions would tend to go in if the steady state were disturbed by a slight increase in $[Ca^{2+}]_i$. The subscripts, i and o, refer to the axoplasm and hemolymph, or internal and external surfaces of the membrane, respectively.

a net charge of 1−) unfilled, and carries three Na^+ ions back on the inward leg. The fact that a 25 mV depolarization may cause less than an e-fold reduction in the Ca efflux (see Fig. 5) might be accounted for if a K^+ sometimes occupied the activator site during the outward journey of the carrier. As mentioned above, a large carrier-independent ("leak") efflux could also contribute to a less than e-fold reduction in Ca efflux per 25 mV depolarization.

The actual net charge on the free carrier is, of course, irrelevant. For example, we may consider an alternative model with an uncharged carrier to which the transported cations are liganded by means of induced-dipole interactions, as occurs in the case of several ionophorous antibiotics (e.g., 23). For this type of carrier, one complete cycle (cf Fig. 14) would also result in the entry of three Na^+ and the exit of one Ca^{2+}. The net entry of one positive charge (as Na^+) is electrically equivalent to the net exit of one negative charge, as proposed for the charged carrier of Fig. 14.

TABLE III. Kinetic Parameters of Na-Ca and Ca-Ca Exchange

	Source of Data				
	Intact Squid Axon		Dialyzed Squid Axon	Crab nerve	Barnacle Muscle
Kinetic Parameter*	Ca Influx (9)	Ca_0-Dependent Na Efflux (9)	Ca Efflux	Ca Influx (24)	Ca Efflux (25)
$K_{Li}(=K_M\dagger)$	–	70 mM	~100 mM†	–	–
$\bar{K}_{Na}$	~75 mM**	(1800 mM)	125 mM†	75 mM	60 mM
K_{Ca_0}	~ 2 mM**	1.8 mM	3 mM†	2 mM	–
K_{Ca_i}	–	–	<0.01 mM‡	–	< 0.001 mM¶

*K_{Li} is the apparent dissociation constant for Li at the external monovalent ion "activator" site (cf Fig. 9 and M^+ of Fig. 14). $\bar{K}_{Na}$ is the apparent half-saturation constant for external Na at the carrier site which presumably binds either $2Na^+$ or Ca^{2+}. The $\bar{K}_{Na}$ value in parentheses (1800 mM) was obtained from a model with slightly different kinetics and is not directly comparable with the kinetics of the model described here. K_{Ca_0} and K_{Ca_i} refer to the apparent dissociation constants for Ca at the outer and inner surfaces of the membrane, respectively.

**Estimated from the Li-Na curve of Fig. 7A, using an equation of the form:

$$v = \frac{V}{\frac{K_{Ca_0}}{1 + [Ca]_0}\left(\frac{[Na]_0}{1 + \bar{K}_{Na}}\right)^2}$$

where v is the Ca influx at any $[Ca]_0$ and V is the maximal Ca influx. The monovalent cation (M^+) binding site was assumed to be saturated at all points on the curve, since $[Na]_0 + [Li]_0$ always totalled 462.5 mM.

†Data obtained in the present study.

‡Estimated from the data of Di Polo (20; Fig. 1). Although these data are from axons dialyzed with fluid containing 5 mM ATP, Di Polo's data indicate that ATP does not influence the $Na_0 + Ca_0$-dependent Ca efflux.

¶Data from internally dialyzed barnacle muscle fibers (Russell and Blaustein, unpublished).

The foregoing considerations involve the interactions between the ions and the carrier, but do not deal with the nature of the exchange. The model shown in Fig. 14 assumes that the carrier shuttles between the internal and external surfaces of the membrane. However, the available data cannot distinguish between this mechanism and a long molecule (an idea first suggested to us by A. L. Hodgkin) which faces both the internal and external environments, and which flips 180° when the appropriate cations on both sides are simultaneously liganded to the carrier.

Kinetic Parameters of the Ca Carrier

Some aspects of the carrier kinetics were examined in the course of these experiments. This information, combined with data from related studies, is summarized in Table III. Included are data from crab nerve (24) and barnacle muscle (25), since these invertebrate preparations appear to have a rather similar Ca transport to that of squid axons – a view which the comparison of data shown in Table III helps to substantiate. Of related interest is the evidence that somewhat similar Na-dependent mechanisms may

be involved in Ca transport in a large variety of vertebrate nerve, muscle, secretory, and epithelial tissues (for a review of this subject, see Ref. 1).

One kinetic parameter which deserves special comment is the dissociation constant for Ca. In order for the Na-Ca exchange carrier to extrude Ca effectively from intact axons, it must be capable of taking up Ca from the internal environment ($[Ca^{2+}]_i \leq 10^{-6}$ M) and depositing the Ca in the extracellular medium ($[Ca^{2+}]_o > 10^{-3}$ M). It seems unlikely that a carrier with a Ca dissociation constant of about 2 to 3 mM (the apparent value at the external site) could bind sufficient Ca at the inner surface to play a significant role in Ca extrusion. The limited information currently available (see Table III) suggests that the affinity of the carrier for Ca at the internal surface may indeed be greater than at the external surface. Our own experience also indicates that the internal Ca-binding site saturates at a rather high pCa, since the Na_o-dependent Ca efflux is increased by no more than about 3- to 5-fold when pCa is decreased from about 6 to less than 4 (e.g., compare Fig. 8 with Figs. 2 and 6). Furthermore, a low value for K_{Ca_i} (the apparent dissociation constant for Ca at the axoplasmic site) of the order of 0.01 mM or less, combined with an apparent half-saturation constant for Na of about 5–50 mM at the inner Na-or-Ca site, could explain the relatively small slope observed for the relationship between $[Na]_i$ and Ca efflux (see Results and Fig. 12) despite a 2Na:1Ca competition. The idea that two Na^+ ions act cooperatively at the inner site stems from the observation that Li_o-simulated Na efflux (which is very nearly equal to the Ca_o-dependent Na efflux) is approximately proportional to the square of $[Na]_i$ (9). Additional indirect support for competition between internal Na and internal Ca comes from the observation that cyanide, which increases $[Ca^{2+}]_i$ (3), abolishes the Li_o -stimulated Na efflux (9).

An interesting feature of the carrier's apparent high affinity for Ca at the inner side of the membrane is its great preference for Ca^{2+} over Mg^{2+}, since the free Mg^{2+} concentration in squid axoplasm is about 2 to 3 mM (26). Certainly the Ca/Mg selectivity ratio for known divalent cation ionophores (e.g., 27, 28) does not even approach the apparent selectivity exhibited here.

Assuming that the Ca and Na fluxes discussed here reflect the operation of a single carrier mechanism, it seems important to learn whether or not the apparent dissociation constant for Ca is in fact different at the two membrane surfaces – as indicated by the data in Table III. If this is the case, an interesting question to be resolved would be the mechanism whereby the affinity for Ca is altered as the carrier rotates or shuttles across the membrane. Baker (19, and unpublished data) has obtained evidence that the apparent dissociation constants for both Na and Ca at the external surface of the squid axolemma may be significantly greater in poisoned axons than in unpoisoned or ATP-injected axons. However, it should be noted that all of the values listed in Table III, with the exception of data from the present series of experiments, were obtained on unpoisoned nerve and muscle preparations. Clearly, more data are needed to resolve this question.

A further complication in the evaluation of these kinetic parameters stems from the probable existence of surface potentials of unequal magnitude at the inner and outer membrane surfaces (cf 29). The presence of diffuse double layers at these surfaces may mean that the absolute and relative concentrations of Na^+ and Ca^{2+} at the membrane surfaces are very different from those in the bulk solutions. At present, it seems best to

ignore this problem, although more detailed evaluation of the kinetic parameters may require that these considerations be taken into account.

On the Energy Required for Ca Translocation

As noted in the Introduction, the observed $[Ca^{2+}]_o/[Ca^{2+}]_i$ gradient in the squid axon is about 10^4. In the steady state, a Ca carrier mechanism which exchanges three Na^+ for one Ca^{2+} should be able to derive sufficient energy from the Na and voltage gradients to support a Ca ratio given by:

$$\frac{[Ca^{2+}]_o}{[Ca^{2+}]_i} = \left(\frac{[Na^+]_o}{[Na^+]_i}\right)^3 \exp \frac{-VF}{RT} \qquad (2)$$

With an Na ratio ($[Na^+]_o/[Na^+]_i$) of about 10 and a membrane potential (V) of about −60 mV, values which are reasonable for intact squid axons (e.g., 30), the calculated Ca ratio is about 10^4. This may mean that the Na and voltage gradients can alone provide an adequate supply of energy to power Ca efflux. The present experiments cannot, however, exclude possible participation of a metabolically driven Ca transport mechanism in the regulation of cell Ca in vivo.

ACKNOWLEDGMENTS

The authors are indebted to the Director and staff of the Marine Biological Laboratory, Woods Hole, Mass., and the Director and staff of the Laboratory of the Marine Biological Association of the U.K., Plymouth, England, for providing excellent facilities and procuring a bountiful supply of squid. Mr. V. Creasy and Mr. R. H. Cook designed and built a number of essential pieces of equipment. Dr. E. Ashare of Fabric Research Laboratories was a great help when problems regarding cellulose acetate fibers cropped up. Dr. P. F. Baker provided much fruitful discussion and collaborated on several of the experiments at Plymouth. Dr. F. J. Brinley, Jr.'s advice and encouragement was indispensable in helping us to master the dialysis techniques. Dr. W. F. Pickard gave invaluable assistance in analysis of the diffusion problems. This research was supported by USPHS (NIH) grants NS-08442 and NS-11223, NSF grant GB-38845, and grants to Dr. P. F. Baker from the Royal Society and the Medical Research Council (U.K.). Dr. Russell was an NINDS postdoctoral fellow.

REFERENCES

1. Blaustein, M. P., Rev. Physiol. Biochem. Pharmacol. 70:33 (1974).
2. Hodgkin, A. L., and Keynes, R. D., J. Physiol. (London) 138:253 (1957).
3. Blaustein, M. P., and Hodgkin, A. L., J. Physiol. (London) 200:497 (1969).
4. Katz, B., and Miledi, R., J. Physiol. (London) 192:407 (1967).
5. Baker, P. F., Hodgkin, A. L., and Ridgeway, E. B., J. Physiol. (London) 218:709 (1972).
6. Baker, P. F., Prog. Biophys. Molec. Biol. 24:177 (1972).
7. Rojas, E., and Hidalgo, C., Biochim. Biophys. Acta 163:550 (1968).
8. Caldwell, P. C., J. Physiol. (London) 152:545 (1960).

9. Baker, P. F., Blaustein, M. P., Hodgkin, A. L., and Steinhardt, R. A., J. Physiol. (London) 200:431 (1969).
10. Brinley, F. J., Jr., and Mullins, L. J., J. Gen. Physiol. 50:2303 (1967).
11. Brinley, F. J., Jr., and Mullins, L. J., Ann. N.Y. Acad. Sci. (in press).
12. Borle, A. B., and Briggs, F. N., Anal. Chem. 40:339 (1968).
13. Portzehl, H., Caldwell, P. C., and Ruegg, J. C., Biochim. Biophys. Acta 79:581 (1964).
14. Ohta, M., Narahashi, T., and Keeler, R. F., J. Pharm. Exper. Therap. 184:143 (1973).
15. Ussing, H. H., Nature 160:262 (1947).
16. Mullins, L. B., and Brinley, F. J., Jr., J. Gen. Physiol. 50:2333 (1967).
17. Hodgkin, A. L., and Keynes, R. D., J. Physiol. (London) 128:28 (1955).
18. Brinley, F. J., Jr., and Mullins, L. B., J. Gen. Physiol. 52:181 (1968).
19. Baker, P. F., and Glitsch, H. G., J. Physiol. (London) 233:44P (1973).
20. Di Polo, R., J. Gen. Physiol. 62:575 (1973).
21. Rosenberg, T., and Wilbrandt, W., J. Gen. Physiol. 41:289 (1957).
22. Wilbrandt, W., and Rosenberg, T., Pharmacol. Rev. 13:109 (1961).
23. Pressman, B. C., Fed. Proc. 27:1283 (1968).
24. Baker, P. F., and Blaustein, M. P., Biochim. Biophys. Acta 150:167 (1968).
25. Russell, J. M., and Blaustein, M. P., J. Gen. Physiol. 63:144 (1974).
26. Baker, P. F., and Crawford, A. C., J. Physiol. (London) 227:855 (1972).
27. Reed, P. W., and Lardy, H. A., J. Biol. Chem. 247:6970 (1972).
28. Pressman, B. C., Fed. Proc. 32:1698 (1973).
29. McLaughlin, S., and Harary, H., Biophys. J. 14:200 (1974).
30. Hodgkin, A. L., Biol. Rev. 26:339 (1951).